Article

A Simple Fluorescent Chemosensor for Detection of Zinc Ions in Some Real Samples and Intracellular Imaging in Living Cells

Ayman A. A. Aziz, [iD] *,a Amir E. Aboelhasan[a] and Mostafa A. Sayed[a]*

[a]Chemistry Department, Faculty of Science, Ain Shams University, Abbassia, 11566 Cairo, Egypt

A new designed fluorescent chemosensor TYMN ((*E*)-1-((thiazol-2-ylimino)methyl) naphthalen-2-ol) for highly sensitive and selective tracing of trace amount of Zn^{2+} ions in some real samples was synthesized and characterized. The sensor TYMN can detect Zn^{2+} ions via fluorescence enhancement with a high selectivity over a wide range of metal ions, especially Cd^{2+}. The sensor showed large fluorescence enhancement upon complexation with Zn^{2+} and simultaneous color change from yellow to orange. The limit of detection was analyzed to be 0.0311 μM with a linear dynamic range 0.1-1.0 μM. The sensor could work in a pH span of 5.0-8.0. Based on the physicochemical and analytical methods like electrospray ionization (ESI)-mass, Job plot, ^1H nuclear magnetic resonance (NMR) and theoretical calculations, the detection mechanism for Zn^{2+} was explained based on restriction of internal charge transfer (ICT) mechanism. TYMN sensor was potentially utilized for Zn^{2+} ions concentration evaluation in some real samples. Fluorescence microscopy experiments revealed that probe TYMN may have application as a fluorophore to detect the Zn^{2+} in living cells.

Keywords: fluorescence, chemosensor, Schiff base, zinc recognition, DFT calculation, fluorescence bioimaging

Introduction

Recently, as a result of concern for human health and environmental safety, worldwide attention has been devoted to design and synthesize highly sensitive fluorescent probes for the selective recognition of heavy metal ions.[1-7] Among the most important natural metal cations, zinc is the second most abundant metal ion that has a large biological spectrum of functions.[8] Abnormal concentration of zinc causes frequent depressed immune function, accustom infections, bullous pustular dermatitis, diarrhea, alopecia, mental disturbances, metal fume fever, adult respiratory distress syndrome.[9,10]

For the important roles of Zn^{2+} ions in biochemistry, there were numerous techniques targeting Zn^{2+} sensing, such as atomic absorption spectroscopy (AAS),[11,12] inductively coupled plasma atomic emission,[13] anodic stripping voltammetry,[14] potentiometry[15] or spectrophotometry.[16] However, the wide utilization of these methods is largely limited due to complicated sample preparation processes, time consuming, high cost, not easily adaptable for online monitoring, low sensitivity and some inherent interference especially with Cd^{2+} ions due to similar chemical properties.

To avoid such drawbacks, and using the special advantages of fluorescence criteria such as its easy performance, high sensitivity, genuine selectivity, fast, simple and real time response,[17,18] various fluorescent probes have been developed for recognition of Zn^{2+} ions.[19-25] Furthermore, for improving either the sensitivity and/or selectivity of Zn^{2+} sensing, Schiff bases as chemosensors have great attention.[26-33]

As an extension of our previous works[34-37] using Schiff bases as chemosensors, in the present work, we present a highly selective and sensitive novel fluorescence probe (*E*)-1-((thiazol-2-ylimino)methyl)naphthalen-2-ol (TYMN) which can detect Zn^{2+} via a fluorescence enhancement.

Experimental

Materials and reagents

All solvents were of reagent grade quality and were supplied from Merck (Darmstadt, Germany). Metal nitrate salts were used for preparation of metal ions solutions. 1 M HEPES (4-(2-hydroxyethyl)-1-piperazineethanesulfonic acid) in H_2O, 2-aminothiazole and 2-hydroxy-1-naphthaldehyde were supplied from Sigma-Aldrich (Saint Louis, MO, USA). TYMN sensor was dissolved in a mixed

aqueous media dimethyl sulfoxide (DMSO):H_2O (v/v, 1:9) to form 1 mM stock solution. Metal salts were dissolved in H_2O to get 10 mM stock solutions. A stock solution of Zn^{2+} (1 mM) was prepared by dissolving 0.02974 g $Zn(NO_3)_2.6H_2O$ in exactly 100 mL of deionized water and standardized with ethylenediamine tetraacetic acid (EDTA).[38]

Characterization methods

Jenway 6270 Fluorimeter was used for recording all fluorescence measurements. pH adjustment was carried out by using Jenway pH meter, model 3510, equipped with glass bodied combination pH electrode (924005). All the experiments were carried out at room temperature of 25 ± 1 °C. Elemental analyses (CHNS) were carried out using JEOL JMS-AX500 elemental analyzer. Fourier transform infrared (FTIR) spectrum of the chemosensor was obtained in KBr discs on a Unicam-Mattson 1000 FTIR. ^1H and ^{13}C nuclear magnetic resonance (NMR) spectra were performed on a Bruker Avance Drx 300-MHz spectrometer with tetramethylsilane (TMS) as an internal standard. Time of flight mass spectrometry (TOF-MS) measurements were carried out on a JEOL JMS-AX 500 spectrometer. Flame atomic absorption spectrometry (FAAS) was used for the determination of zinc concentration at a wavelength of 213.9 nm, 30 mA, band width 0.7 nm and air-acetylene gas. Microwave synthesis was performed in open glass vessel on a modified microwave oven model 2001 ETB with rotating tray and a power source 230 V, microwave energy output 800 W and microwave frequency 2450 MHz. The surface morphology of the samples was evaluated by a scanning electron microscope (SEM, XL 30 ESEM, Philips) set at 20 kV. Prior to the examination, the samples were sputter coated with gold-palladium under argon atmosphere.

Microwave assisted sensor synthesis of TMYN and characterization data

As shown in Scheme 1, the novel sensor, (*E*)-3-((thiazol-2-ylimino)methyl)naphthalen-2-ol (TYMN), was prepared according to the literature,[39] with some modification under the effect of microwave radiation. A homogeneous mixture of 2-aminothiazole (2.0 g, 20 mmol), 2-hydroxy-
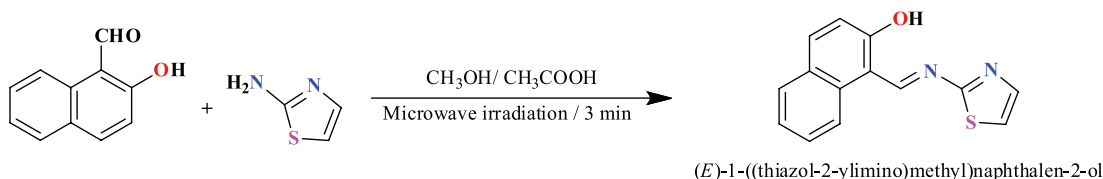
1-naphthaldehyde (3.4 g, 20 mmol), acetic acid (0.2 mL) in methanol (10 mL), was put in a microwave reaction vessel equipped with a magnetic stirrer. The vessel was closed, and the reaction was irradiated at 50 W for 30 s interval for 3 min. The solid was washed by aqueous sodium bisulfite solution and purified by recrystallization. FTIR and ^{13}C NMR spectra are depicted in Supplementary Information section as Figures S1 and S2.

Characteristics of TYMN were as follows: ($C_{14}H_{10}N_2OS$) molecular weight / (g mol^{-1}) 254.31; yield: 86%; mp 171-173 °C; color: yellow; IR (KBr) ν / cm^{-1} 3430, 1610, 1221, 712; ^1H NMR (400 MHz, DMSO) δ 13.82 (s, 1H, OH), 8.62 (s, 1H, CH=N), 7.21-8.62 (m, 6H, aromatic, 2H, thiazole); ^{13}C NMR (300 MHz, DMSO) δ 103.72, 109.53, 122.89, 125.39, 125.73, 128.63, 128.86, 130.31, 134.58, 135.82, 139.60, 142.41, 149.73, 174.65; TOF-MS *m/z*, calcd. for $C_{14}H_{10}N_2OS$ [M + H]$^+$: 255.47, found: 255.25. Elemental analysis calcd.: C, 66.12; H, 3.96; N, 11.02; S, 12.61%; found: C, 67.00; H, 3.59; N, 11.10; S, 12.31%.

Quantum yield measurement

The fluorescence quantum yield ϕ_S of TYMN chemosensor in EtOH was calculated employing the comparative William's method which involves the use of well-characterized standards with known quantum yield (ϕ_R) values.[40] From the absorption and fluorescence spectra of probe, the quantum yield (ϕ_S) values were calculated according to equation 1:[41]

$$\phi_S = \phi_R \frac{A_R}{A_S} \frac{I_R}{I_S} \frac{\eta_R^2}{\eta_S^2} \tag{1}$$

where S and R stand for the sample and reference (quinine sulfate, $\phi_R = 0.54$ in 0.05 M H_2SO_4),[42] respectively; A represents the absorbance at the excitation wavelength; I refers to the integrated emission band areas at the excitation wavelength (360 nm), and η is the solvent refractive index.

General procedures for fluorogenic detection of Zn^{2+} using TYMN probe

To 10 mL volumetric flasks containing different amounts of zinc ions, 1.0 mL of TYMN (10 μM) was

Scheme 1. Synthesis of probe TYMN ((*E*)-1-((thiazol-2-ylimino)methyl)naphthalen-2-ol).

added directly, then the flask was completed to the mark by HEPES buffer solution (pH 7.0). After shaking for 10 s and waiting for about 5 min at room temperature, 3 mL of the solution was put into the fluorescent cell and the fluorescence intensity was recorded immediately at an emission wavelength of 360 nm. Each value was mean of three replicates.

Sample preparation

Fruits and vegetable sample

Fruits and vegetable samples (apple, grape, tomato and potato) were collected from the local market with plastic bags. The samples were rinsed in distilled water to remove dust and adhered particles, dried in an oven at ca. 60 °C, crushed with a porcelain mortar, and stored in double-cup polyethylene bottles. 2.0 g of the dried sample was transferred to a clean beaker and digested in 10 mL of a concentrated HNO_3 (70%) by using a hotplate for ca. 30 min. The mixture was filtered through a 0.45-mm filter paper, after cooling at room temperature. The aliquot was quantitatively transferred to a 50 mL volumetric flask and completed with deionized water for analysis.

Pharmaceutical samples

Vitazinc (capsules)

A Vitazinc capsule was dissolved in about 5 mL aqua regia and the solution was evaporated to dryness. The process was repeated, then dissolved in 10 mL of deionized water and transferred quantitatively into 100 mL volumetric flask and completed with HEPES buffer (pH 7.0).

Calamine lotion

1 mL portion of the lotion was dissolved in 10 mL of 2 M HNO_3 and heated for several minutes to near boiling, then cooled, filtered and transferred quantitatively into 50 mL volumetric flask. The flask was then completed by HEPES buffer solution (pH 7.0).

3-(4,5-Dimethylthiazole-2-yl)-2,5-diphenyl tetrazolium bromide (MTT) assay

The cell viability of the probe TYMN was tested against the living HeLa cell lines using the 3-(4,5-dimethylthiazole-2-yl)-2,5-diphenyl tetrazolium bromide (MTT) assay. The cells were seeded into a well plate at a density of 1.5×10^4 cells _per_ well and incubated in medium containing TYMN at concentrations ranging from 0 to 50 μM for 30 min. To each well, 100 μL of MTT was added and the plates were incubated at 37 °C for 1 h to allow MTT to form formazan crystals by reacting with metabolically active cells. The medium with MTT was removed from the wells. Intracellular formazan crystals were dissolved by adding 100 μL of DMSO to each well and the plates were shaken for 10 min. The absorbance was recorded using plate reader (Multiskan EX; Thermo Fisher Scientific Inc., Waltham, MA, USA).

Cell culture and fluorescence bio-imaging

TYMN sensor was used for _in vitro_ fluorescence imaging of zinc in HeLa cells. Dulbecco's modified Eagle's medium (DMEM) containing 10% fetal bovine serum (FBS) was used to maintain the living HeLa cells at 37 °C in a humidified incubator provided with 5% CO_2. Afterward, the cells were washed with HEPES buffer for several times to remove the residual DMEM medium and dead cells. In HEPES buffer, pH = 7.0, holding 1% DMSO as co-solvent for 30 min at 37 °C, HeLa cells were incubated with TYMN (10.0 μM). To eradicate excess of TYMN in the extracellular medium, the incubated cells were swabbed with HEPES for several times. To eradicate excess of TYMN in the extracellular medium, the incubated cells were swabbed with HEPES for several times, then subjected to fluorescence imaging. The HeLa cells were then further allowed to incubate with with Zn^{2+} (20 μM in HEPES buffer) for 10 min at 37 °C and were then subjected to fluorescence imaging using a CarlZeiss LSM 710 confocal microscope system (Germany)

Results and Discussion

The Schiff base (TYMN) was designed and green synthesized by condensation between 2-hydroxy-1-naphthaldehyde and 2-aminothiazole under microwave conditions in high yields. Its structure was confirmed by FTIR, ^{1}H NMR, ^{13}C NMR, TOF-MS and X-ray analysis. The full crystallographic data can be found in our previous work.[39]

Morphology of TYMN and its Zn[II] complex

The morphological properties of TYMN and its Zn^{2+} complex were characterized by SEM. The SEM micrographs are depicted in Figure 1. The SEM analysis provides a strong evidence for Zn^{2+} coordination to TYMN via significant changes in the surface morphology. The SEM micrograph of TYMN sensor demonstrates nonuniform platelet-like structure associated with variable lateral dimensions. On contrast, the SEM micrographs of TYMN-Zn complex exhibits a tube-like morphology.

Moreover, uniform matrix of the synthesized Zn complex was clearly noticed in the pictograph.
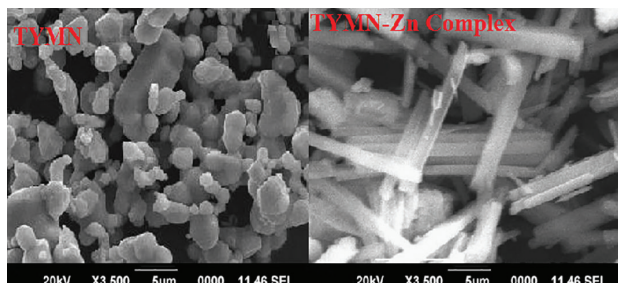
Figure 1. Scanning electron microscopy images of TYMN and TYMN-Zn complex.

Photophysical properties of TYMN sensor

The affinity of the TYMN sensor towards numerous metal ions was performed by recording UV-Vis absorption and emission spectra in mixed solvent DMSO/H_2O system (v/v, 1:9, 5 mM, HEPES buffer, pH 7.0), where DMSO was used as a co-solvent. As shown in Figure 2, the absorption spectrum of TYMN (5.0 μM) exhibited two bands, at 316 nm which can be attributed to π-π* transition of the conjugated system including benzene ring and the double bond of the azomethine group and at 356 nm due to n-π* transition of non-bonding electrons present on the nitrogen of the azomethine group. Upon addition of 5.0 μM Zn^{2+} (1 equivalent), a new absorption signal appeared at 469 nm with color change of TYMN color from yellow to orange (Figure 2 inset). The formation of new absorption band was ascribed to the formation of TYMN-Zn complex with different color from that of the sensor. On the contrary, addition of other competitive metal ions, such as Co^{2+}, Ni^{2+},
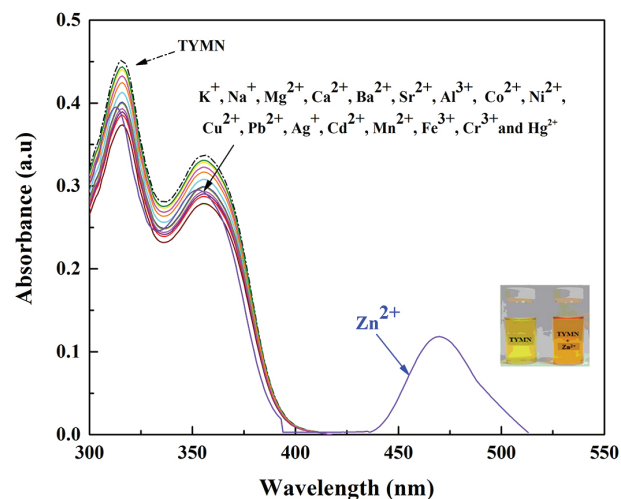
Figure 2. Absorption spectra of TYMN (10 μM) in 10% (v/v) DMSO/H_2O buffered by 5 mM HEPES at pH 7.0 at 25 °C, upon addition of various 5 equiv. metal ions.

Cu^{2+}, Pb^{2+}, Ag^+, Cd^{2+}, Mn^{2+}, Fe^{3+}, Cr^{3+}, Hg^{2+}, K^+, Na^+, Mg^{2+}, Ca^{2+}, Ba^{2+}, Sr^{2+}, and Al^{3+}, no intrinsic absorbance changes were observed. The results demonstrated that TYMN is characteristic of high selectivity toward Zn^{2+} over other competitive metal ions.

TYMN sensor fluorescence properties were evaluated with distinguished metal ions in DMSO/H_2O system (v/v, 1:9, 50 mM HEPES, pH 7.0) at 25 °C. The sole sensor TYMN (10 μM) exhibited a weak characteristic fluorescence emission at 586 nm (quantum yield, Φ = 0.026), upon excitation at wavelength 360 nm (Figure 3). The weak fluorescence intensity may be attributed to internal charge transfer which quench the sensor fluorescence emission. As shown in Figure 3, upon addition of various metal ions, the emission spectra of TYMN nearly did not alter, except on exposure to Zn^{2+} (10 μM), the emission profile shows a specific enhancement in the fluorescence intensity, demonstrating that TYMN behaves as an efficient and selective sensor for Zn^{2+} over other competitive essential metal ions tested.
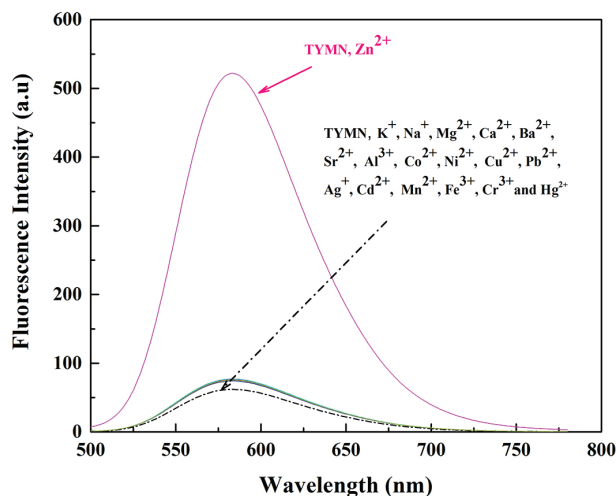
Figure 3. Fluorescence spectra of TYMN sensor (5.0 μM, λ_{ex} = 360 nm, λ_{em} = 583 nm) in presence of some essential metal ions (DMSO/H_2O, v/v, 1:9; 5 mM, HEPES buffer: pH 7.0).

Effect of pH on Zn^{2+} binding with TYMN

The applicability of the TYMN sensor under physiological conditions was checked by investigation of the influence of pH on fluorescence response of TYMN sensor to Zn^{2+} ions at different pH at λ_{em} = 583 nm.[43] The effect of pH on the fluorescence response of TYMN probe and its Zn^{2+} complex was investigated in DMSO/H_2O (1:9, v/v) mixture (Figure 4). The pH of solution was regulated by buffers of KCl/HCl (pH 1.0-2.0), CH_3COOH/NaOH (pH 3.0-4.0), MES (2-(*N*-morpholino) ethanesulfonic acid)/NaOH (pH 4.5-6.0), HEPES

(pH 6.5-9.0) and Tris/NaOH (pH 10.0-12.0). The results showed that the fluorescence profile of TYMN individually does not undergo any noticeable change, whereas in presence of Zn^{2+} ion, the fluorescence intensity was enhanced. At pH > 3.0, the fluorescence emission intensity of TYMN-Zn significantly increases and remain constant in the range 5.0-8.0 and then begin to decrease again, because of phenolic-OH deprotonation and availability of lone pair on azomethine nitrogen atom. The decrease in fluorescence response of TYMN probe at pH < 5.0 arises from proton binding by imine nitrogen.[44] On the other hand, the receded decreases in fluorescence response at pH > 8.0 could be attributed to the formation of Zn^{2+} ion hydroxides.[45] Hence, HEPES buffer solution (pH 7.0) was chosen as the working moiety for further studies.
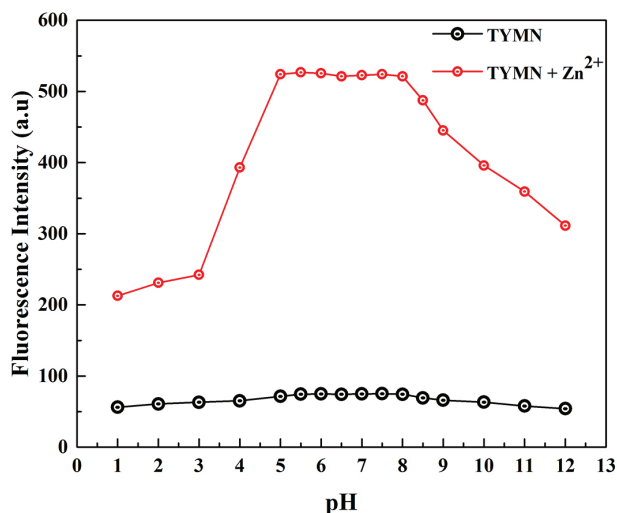
Figure 4. Fluorescence intensities (λ_{ex} = 360 nm, λ_{em} = 583 nm) of TYMN (10.0 μM) in the absence (black plots) and presence (red plots) of Zn^{2+} (5 equiv.) at various pH values.

Response time

For real time applications, as a crucial factor, TYMN fluorescence response in absence and in presence of Zn^{2+} ions were correlated with a time course at an emission wavelength of 583 nm at ordinary room temperature. As shown in Figure 5 with the increase of the reaction time, the fluorescence intensity of TYMN sensor with Zn^{2+} increased and reached equilibrium within 5 min and then almost no change in the fluorescence intensity within 1 h was observed. These indicated that sensor TYMN could serve as an efficient probe for Zn^{2+} quickly and reliably.

Sensitivity and limit of detection (LOD)

To address the sensitivity, TYMN fluorescence responses along with increasing Zn^{2+} ion concentration were

investigated (Figure 6). The results indicated that, upon subsequent gradual increase in Zn^{2+} ion concentration in the range 1.0 to 10 μM, fluorescence intensity increases in a dramatic manner. A linear plot was constructed with average values of the intensities against the concentration of Zn^{2+} ions for determining the slope (Figure 7). The limit of detection was estimated to be 0.0311 on the base of the equation (LOD = $3S_b$ / S, n = 10), and a precision of 3.2% relative standard deviation (RSD) were achieved,[46] where S_b is the standard deviation of the blank solution and S is the slope between fluorescence intensity *versus* sample concentration.
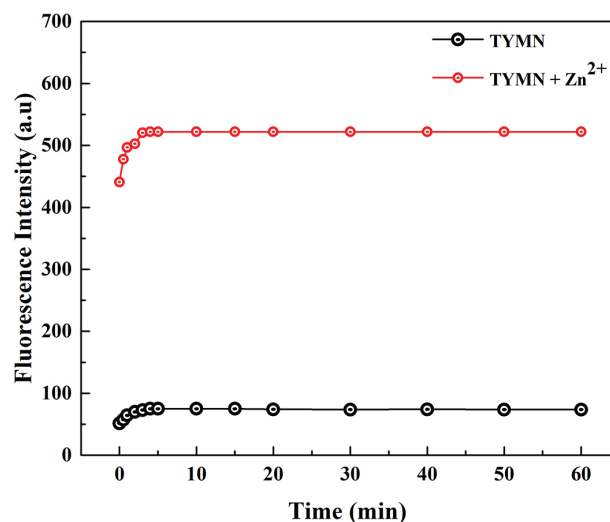
Figure 5. Effect of time on the fluorescence intensity of TYMN (10.0 μM) in absence of Zn^{2+} and in presence of Zn^{2+} ion (5 equiv.) (λ_{ex} = 360 nm, λ_{em} = 583 nm).
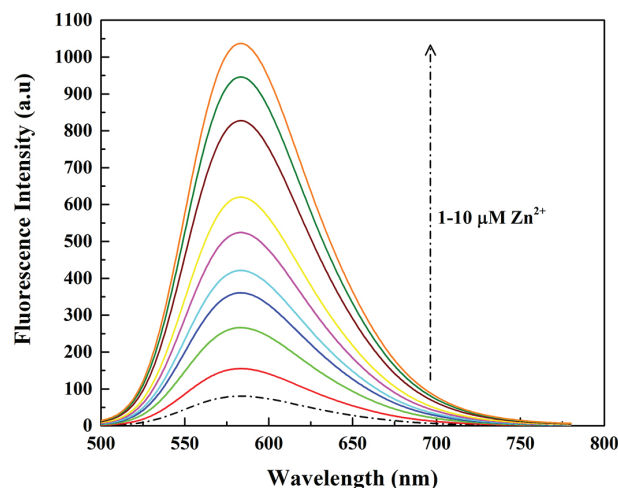
Figure 6. Fluorescence response of sensor TYMN (10 μM) titrated with 0.0-1.0 equiv. of Zn^{2+} solutions in DMSO/H_2O (v/v, 1:9, 0.05 mM HEPES, pH 7.0) solutions (λ_{ex} = 360 nm, λ_{em} = 583 nm).

TYMN sensor selectivity

To demonstrate the practical applicability of the TYMN-Zn fluorescence sensing system, potential
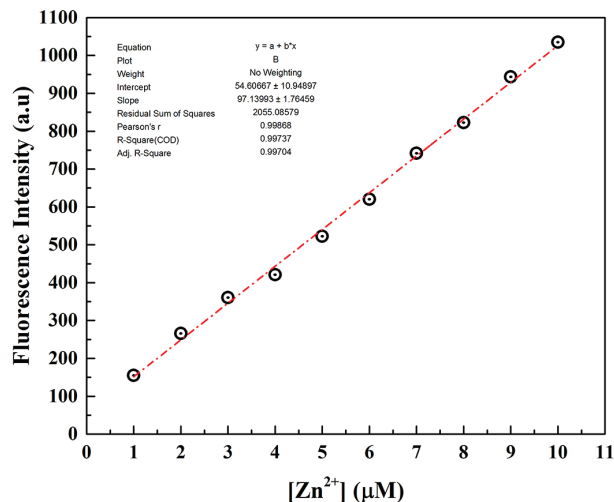
Figure 7. Calibration curve of TYMN-Zn complex (λ_{ex} = 360 nm, λ_{em} = 583 nm).

interferences from the more importantly coexisting species frequently encountered in environmental and biological sample matrices were investigated. The selectivity of TYMN (5 μM) towards the competing ions (50 μM) were investigated in DMSO/H$_2$O (v/v, 1:9, 0.05 mM HEPES, pH 7.0) solutions in the absence (as a blank control) and presence of Zn^{2+} (10 μM). The selectivity of TYMN probe towards the studied metal ions was identified by calculating relative error RE (%) = [(F − F$_0$) / F$_0$] × 100, where F$_0$ and F are the fluorescence intensity in absence and in presence of some interfering ion. Figure 8 demonstrated that the observed relative error was considered as tolerable, reflecting the low interference and high selectivity of the proposed probe.

TYMN sensor reversibility and cyclicity indexes

For practical applications, reversibility and circularity
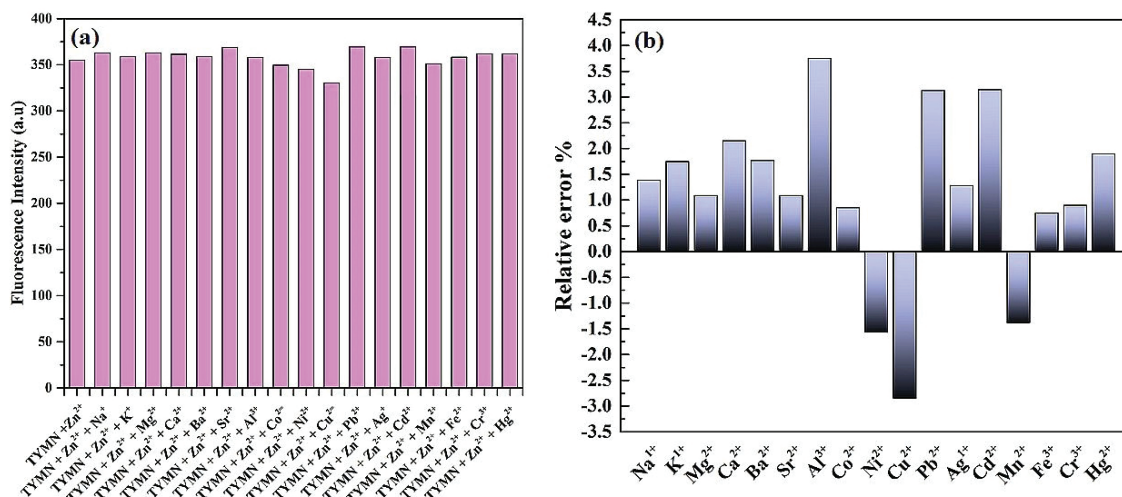
of TYMN-Zn complex were investigated by titration with EDTA. To investigate whether the enhancement of fluorescence emission intensity was actually assigned to Zn^{2+} ion binding with TYMN instead of photoactivation of TYMN sensor, the sensor reversibility study was performed. As seen in the Figure 9a, upon addition of EDTA to the solution containing TYMN-Zn complex, the fluorescence gradually diminished and when [EDTA] is equivalent to [Zn^{2+}], the fluorescence emission signal was restored to lower level of TYMN at 583 nm, indicating regeneration of free TYMN. This inspection predicts that the complexation between Zn^{2+} and TYMN sensor is chemically reversible. Besides, the subsequent addition of Zn^{2+} ions to TYMN solution enhances fluorescence emission. This reversible enhancement process could be repeated at least five times with a little loss of fluorescent intensity (Figure 9b). These results suggested that the recognition process of TYMN probe between Zn^{2+} and EDTA is circularity reversible.

TYMN binding mode with Zn^{2+} ion

Sensing mechanism speculation

As illustrated in Scheme 2, in the absence of Zn^{2+} ions, TYMN fluorophore undergoes intramolecular charge transfer (ICT) from the donor to the acceptor upon photo-excitation, but in the presence of Zn^{2+} ions, the increase in the fluorescence intensity of TYMN can be ascribed to leakage of conjugation as a result of formation of coordinate bonds between O atom of hydroxyl group and the azomethine nitrogen atom, resulting in restriction of photo-induced ICT mechanism.[47,48] Such mechanism causing remarkable fluorescence enhancement was previously reported.[49]

Figure 8. (a) Effects of coexisting ions (5 μM) onto the fluorescence emission of TYMN-Zn (5 μM) in DMSO/H$_2$O at pH 7.0 (λex: 360 nm, λem: 583 nm); (b) selectivity of TYMN probe in terms of relative error (RE).
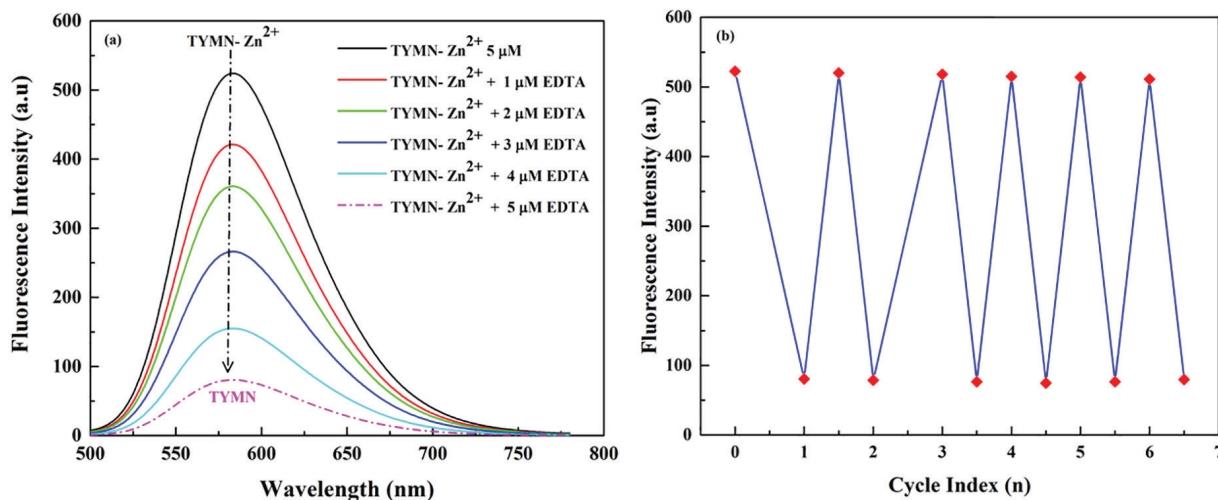
Figure 9. (a) Fluorescence spectra of TYMN-Zn (5 μM) in the absence and presence of EDTA (1-5 μM) in 10% (v/v) DMSO/H₂O buffered by 5 mM HEPES at pH 7.0 at 25 °C (λ_{ex} = 360 nm, λ_{em} = 583 nm); (b) cycle index of TYMN-Zn (5.0 μM) reacting with EDTA (5.0 μM).
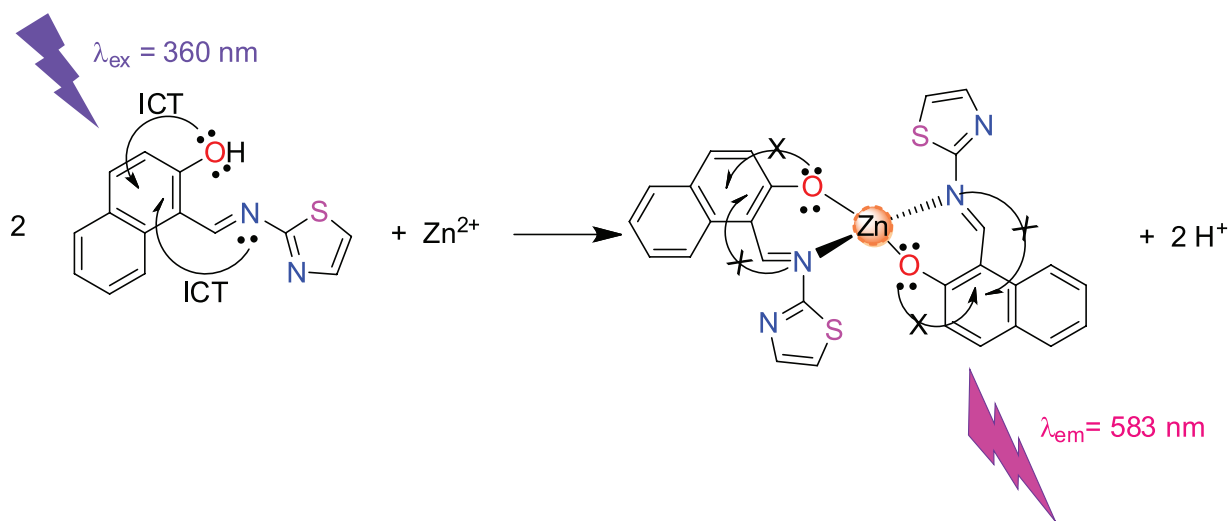
Scheme 2. The proposed binding model for the interaction between TYMN and Zn²⁺ ion.

Stoichiometry stability constant of the TYMN-Zn complex

Using fluorometric titration, the stoichiometry between TYMN and Zn²⁺ was evaluated by Job's plot.[50] The total concentration of TYMN and Zn²⁺ was kept constant in DMSO/H₂O, HEPES-buffer, pH 7.0 system, whereas mole fraction of Zn²⁺ ion was varied continuously. Figure 10 showed that maximum emission was achieved at 0.33 mol fraction of Zn²⁺, indicating 2:1 binding stoichiometry of the complex formed between TYMN and Zn²⁺ ion.

Determination of binding constant

The stoichiometry of TYMN-Zn complex was also confirmed by the Benesi-Hildebrand method.[51] The binding constant of the TYMN-Zn complex formed in solution was calculated by using the standard Benesi-Hildebrand equation.[52-54]

$$\frac{F_{max} - F_0}{F - F_0} = \frac{1}{K_a \left[Zn^{2+} \right]^2} \tag{2}$$

where, F_0 is the fluorescence intensity of free sensor TYMN; F is the observed fluorescence intensity at any given concentration of Zn²⁺ in micromolar; F_{max} is the intensity at saturation point (large excess) with the Zn²⁺; and K_a is the association constant (M⁻²). K_a was determined graphically by plotting $(F_{max} - F_0) / (F - F_0)$ *versus* $1 / [Zn^{2+}]^2$ (Figure 11). As shown in Figure 11 the data showed a good linear relationship with linear fitting with slope = $K_a = 6.6099 \times 10^{10}$. This value fits in the binding constants reported for Zn²⁺ in literature (1.0-10¹²).[55]

TOF-MS-ESI⁺ mass

The suggested stoichiometry of TYMN-Zn complex was corroborated with the data acquired from TOF-MS-ESI⁺
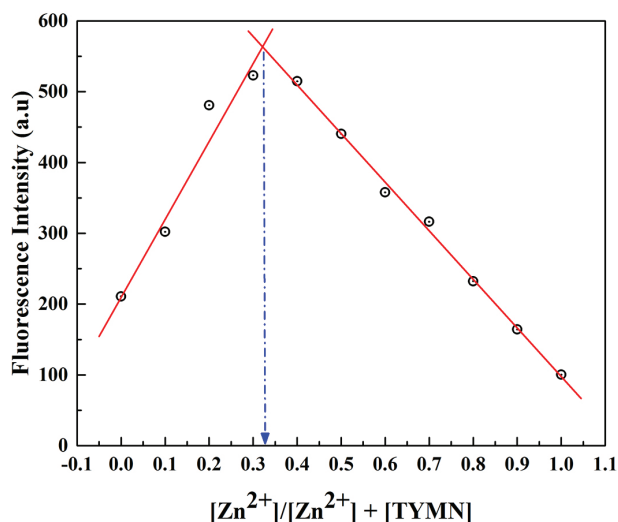
Figure 10. Job's plot for TYMN and Zn^{2+} ([TYMN] + [Zn^{2+}] = 10 μM) in 10% (v/v) $DMSO/H_2O$ buffered by 5 mM HEPES at pH 7.0.
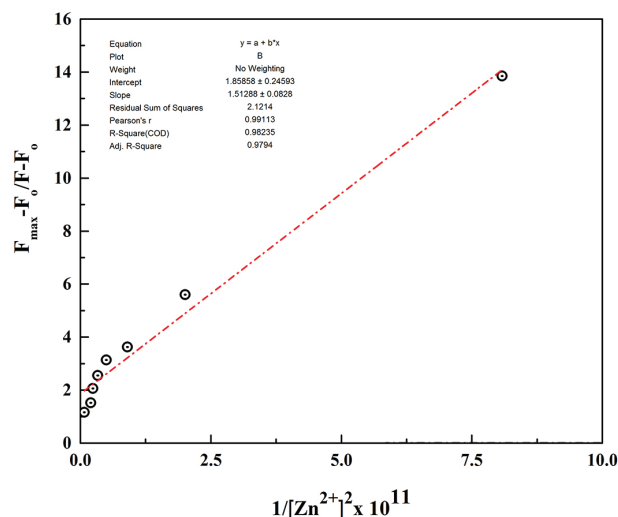
Figure 11. Benesi-Hildebrand plot for determination of TYMN-Zn association constant in $DMSO/H_2O$ (1/9, v/v) (λ_{ex}: 360 nm and λ_{ex}: 583 nm).

electrospray ionization (ESI) mass analysis. Upon addition of Zn^{2+} (2 equiv.) to TYMN, the positive-ion mass spectrum of TYMN exhibited an intense prominent peak at *m/z* 572.04, equivalent to the ion [$Zn(L)_2$] (Figure 12) and reflecting the 1:2 binding stoichiometry of TYMN with Zn^{2+}.

^{1}H NMR titration

Additionally, to better elucidate the complexation behavior of TYMN towards Zn^{2+} ions, ^{1}H NMR titration experiments were performed in DMSO-d_6. The spectral differences for free TYMN and in presence of Zn^{2+} are depicted in Figure 13. The ^{1}H NMR spectra showed fading of OH signal in free probe (δ 13.67 ppm) upon addition of Zn^{2+} ions. This signal completely disappeared upon addition of 2.0 equiv. of Zn^{2+} ions, confirming the induced

deprotonation where the coordination of Zn^{2+} ion to TYMN via the oxygen of the hydroxyl group. Additionally, the coordination of azomethine nitrogen to the Zn^{2+} was indorsed by up-field shift the azomethine proton signal from δ 8.74 to 8.36 ppm.[56] Meanwhile, the aromatic protons multiplet displayed down field shift in the range δ 7.80-8.15 ppm compared to δ 7.21-7.61 ppm from those of free TYMN.

Theoretical studies

Density functional theory (DFT) calculations were performed for TYMN and TYMN-Zn^{2+} using DFT/B3LYP-6-31G basis set model,[57] to gain insight into the fluorescence enhancement of TYMN after Zn^{2+} binding.

The calculations have shown that, the most stable model (energy = 13.97 kcal mol^{-1}) displayed explicit features, with planar conformation and absence of intramolecular hydrogen bonding to any of the nitrogen and sulfur atoms, consistent with the crystal structural analysis.

Furthermore, coordination of Zn^{2+} ion through the nitrogen of the azomethine and the hydroxyl group was supported based on the orientation of the functional groups of TYMN. Additionally, both the X-ray[39] and the theoretical analyses of the TYMN probe supported that TYMN could coordinate to metal as bidentate ligand. Finally, for TYMN-Zn complex, theoretical analysis suggested a minimum tetrahedral geometry with an energy of 265.70 kcal mol^{-1}, 1.92 and 1.88 Å for Zn−N and Zn−O bond distances, respectively.[39]

Comparison of TYMN with recently reported probes

The sensing ability of the developed TYMN probe for Zn^{2+} ion was compared to the various reported methods (Table 1). Comparing with LOD of other probes, it is clearly delineated the proposed probe shows better sensitivity for identification of Zn^{2+} trace amounts in real samples and best selectivity for Zn^{2+} quantification even in presence of Cd^{2+} ions.

Applicability of the sensor in real samples

To investigate the practical use of TYMN sensor in complex matrices, attempts were made to determine Zn^{2+} ions in some real samples including fruits, vegetables and pharmaceuticals samples. A comparison between results obtained by proposed method and FAAS was performed, for evaluating the accuracy of the proposed procedure. As can be seen in Table 2, a good agreement between the results for both methods was obtained.
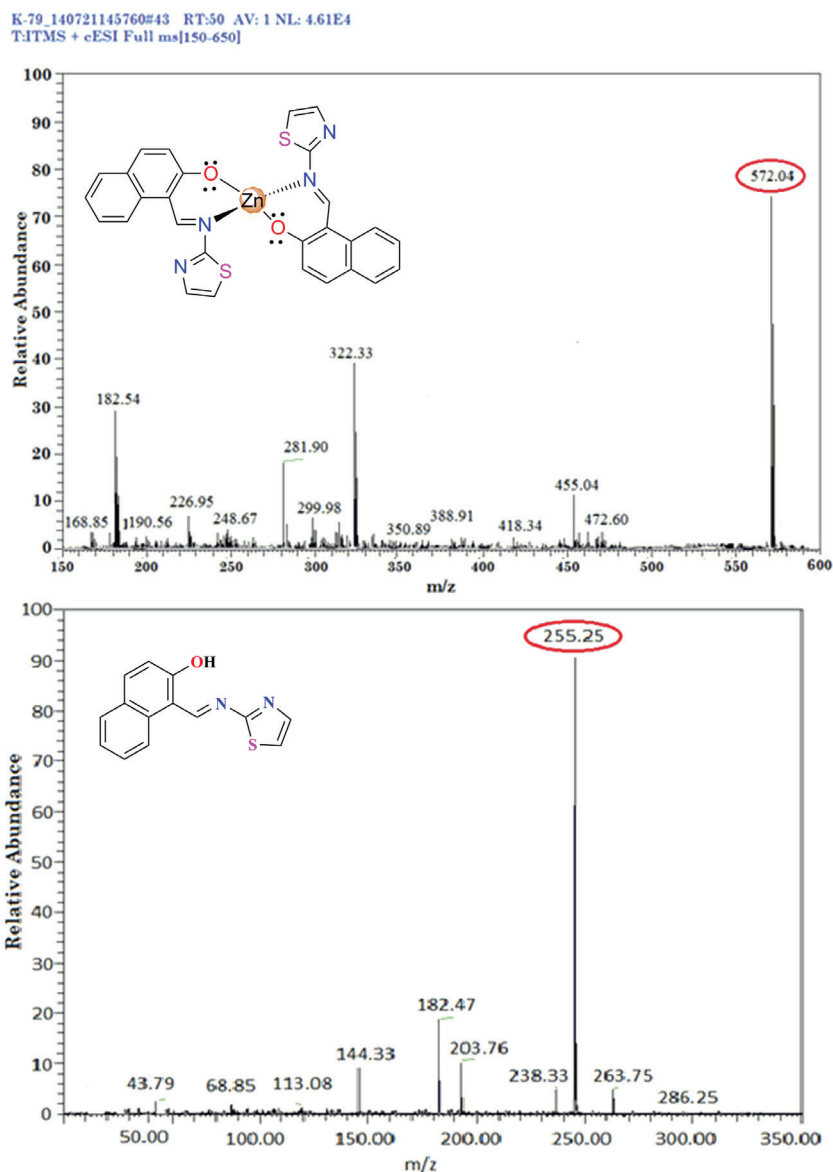
Figure 12. TOF-MS spectra of TYMN probe upon addition of Zn^{2+} ion (2 equiv.) in DMSO.

Application in living cells

Cytotoxicity of TYMN probe

The MTT assay was used to study the cytotoxicity of TYMN probe to HeLa cells during the staining process (Figure 14). As shown in Figure 14a, the dose dependent assay carried out for 1 h of incubation period, 10 μM TYMN, did not show significant cytotoxic effects on HeLa cells, which suggests that TYMN can be readily used for cellular application at the indicated dose. Additionally, the cell viability assay at various time intervals of HeLa cell lines incubated with TYMN (10 μM) (Figure 14b) demonstrates that to a time course of 24 h the cell viability rate is quite stable and only a small percentage loss of cell lines was noted. Thus, an optimal concentration of 10 μM of

TYMN with an incubation period below 1 h was followed in all the confocal imaging studies.

Bioimaging of Zn^{2+} in HeLa cells

The high sensitivity, excellent selectivity, and low cell cytotoxicity of TYMN probe, open the door for potential biological application of TYMN for fluorescence imaging to detect Zn^{2+} in HeLa cells. As shown in Figures 15a-15c, in Dulbecco's modified Eagle's medium supplemented with 10% fetal bovine serum, HeLa cells incubated with TYMN probe solution (10 μM) in 30 min at 37 °C showed a weak fluorescence. On the other hand, treating TYMN-loaded cells with Zn^{2+} (20 μM) drastically enhance fluorescence (Figures 15d-15f) and induces strong fluorescence in the green channel. These observations indicate that TYMN
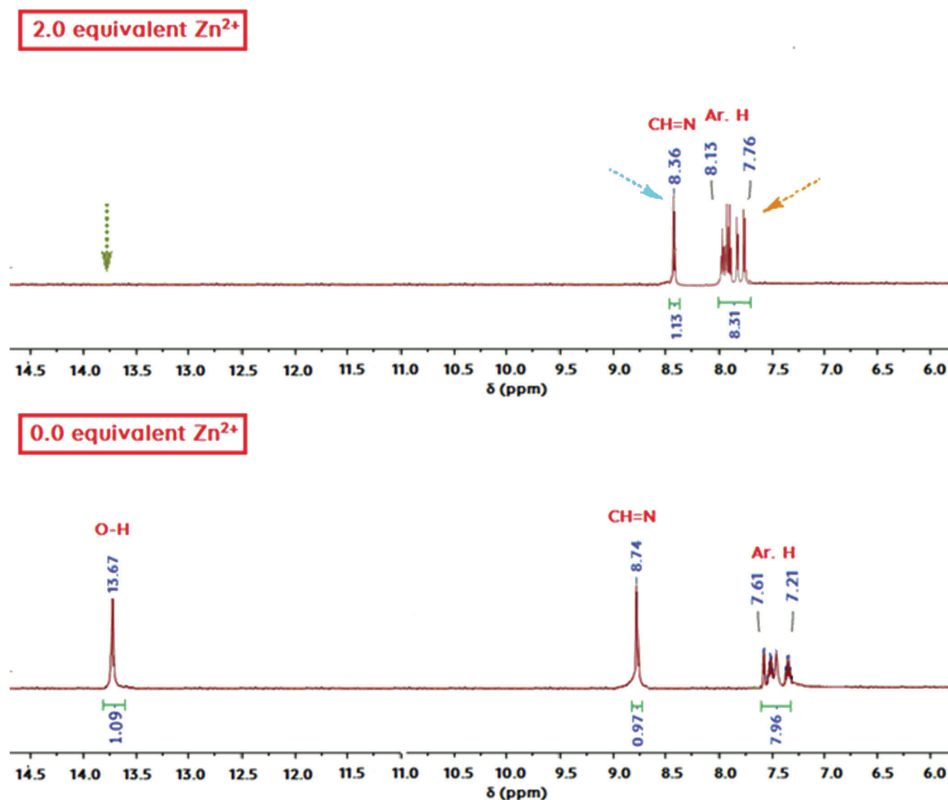
Figure 13. Partial ^{1}H NMR (300 MHz, DMSO-d_6) spectra of TYMN probe in absence (bottom) and in presence (top) of different Zn^{2+} equivalents.

Table 1. Comparison between the proposed probe and some recently reported simple probes for Zn^{2+} detection

No.	Probe	LOD / μM	Reference
1	1-hydroxy-2-naphthaldehyde-2-pyridinehydrazone derivatives	0.17	27
2	(E)-N'-(5-allyl-2-hydroxy-3-methoxybenzylidene)nicotinohydrazide	4.35 × 10^{-3}	28
3	(E)-N'-(2-hydroxybenzylidene)-3,5-di-*tert*-butyl-2-hydroxybenzo hydrazide	2.83	29
4	3-(benzo[*d*]thiazol-2-yl)-4-hydroxy-2*H*-chromen-2-one	0.358	30
5	furan-2-carbohydrazide-5-(2-thienyl)-salicylaldehyde	0.77	31
6	N,N'-phenylenebis(salicylideaminato)	0.15	32
7	pyridoxal-2-hydrazinopyridine Schiff-base	0.07	33
8	(E)-3-((thiazol-2-ylimino)methyl)naphthalen-2-ol	0.0311	current method

LOD: limit of detection.

Table 2. Determination of zinc in real samples (n = 6)

Sample	Amount of zinc (mean ± SD)		Relative error / %
	FAAS	Present method	
Apple / (mg kg^{-1})	6.1 ± 0.19	6.2 ± 0.8	−1.63
Grape / (mg kg^{-1})	5.7 ± 0.13	5.6 ± 0.72	1.75
Tomato / (mg kg^{-1})	2.7 ± 0.06	2.8 ± 0.03	−3.70
Potato / (mg kg^{-1})	4.06 ± 0.37	4.11 ± 0.22	−1.23
Vitazinc capsules / (mg *per* capsule)	25.05 ± 0.98	24.97 ± 0.77	0.319
Calamine lotion / (mg mL^{-1})	8.06 ± 0.13	8.00 ± 0.16	0.744

SD: standard deviation; FAAS: flame atomic absorption spectrometry.
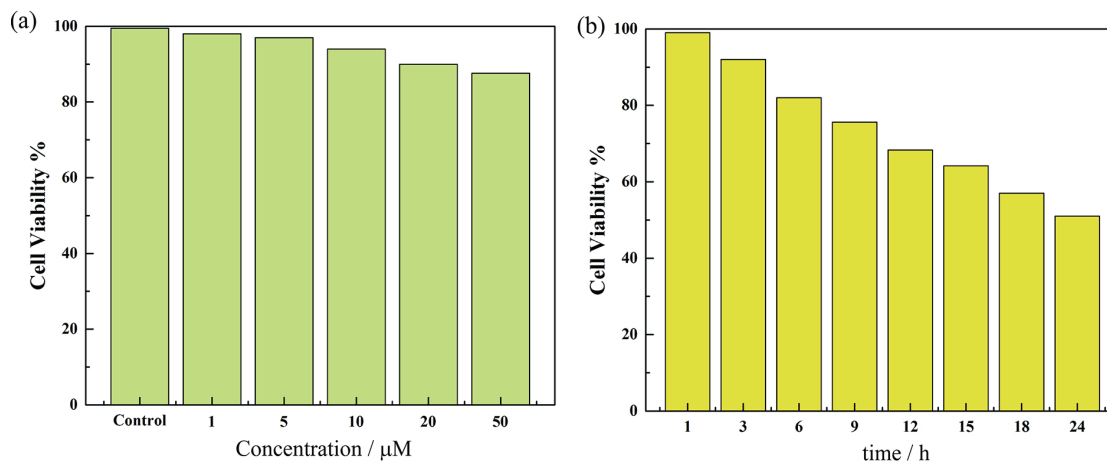
Figure 14. (a) Cytotoxicity of TYMN probe at varying concentration dependent assay; (b) cytotoxicity of TYMN probe at varying time dependent assay.
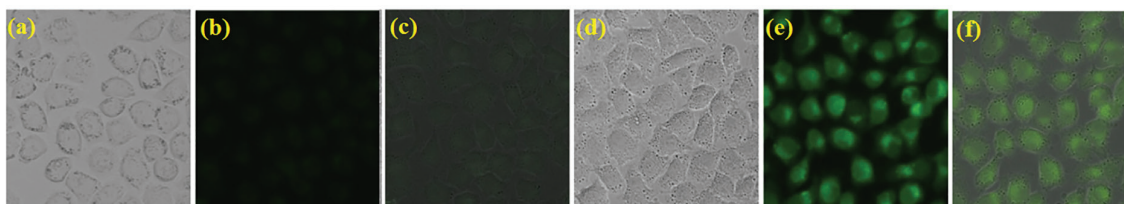
Figure 15. (a) Bright field, (b) fluorescence and (c) overlay images of HeLa cells stained with 10 μM of TYMN; (d) bright field, (e) fluorescence and (f) overlay images of HeLa cells stained with 10 μM of TYMN then with 20 μM Zn^{2+}.

probe had good cell-membrane permeability, which could be used for detecting Zn^{2+} *in vivo*.

Conclusions

A new Schiff base fluorophore (TYMN) for detection of zinc ions was designed, synthesized and characterized. A 1:2 stoichiometry between TYMN and Zn^{2+} was demonstrated by Job's plot. The probe could rapidly respond to Zn^{2+} with a high selectivity (LOD = 0.0311 μM), which allows detection of zinc ions in biological and environmental samples. All biologically relevant metal ions and toxic heavy metals did not interfere with the Zn^{2+} ion detection with this sensor. Most significantly, fluorescence cell imaging experiments revealed that TYMN sensor has good cell-membrane permeability and can be used as a marker for sensing Zn^{2+} in living cells.

Supplementary Information

Supplementary data (FTIR, ^{13}C NMR spectra) are available free of charge at http://jbcs.sbq.org.br as PDF file.

Acknowledgments

References

1. Carter, K. P.; Young, A. M.; Palmer, A. E.; *Chem. Rev.* **2014**, *114*, 4564; Zhu, H.; Fan, J.; Wang, B.; Peng, X.; *Chem. Soc. Rev.* **2015**, *44*, 4337.

2. Patil, A.; Gawali, S. S.; *Inorg. Chim. Acta* **2018**, *482*, 99.

3. Şenkuytu, E.; Eçik, E. T.; Çoşut, B.; *J. Lumin.* **2018**, *203*, 639.

4. Anand, T.; Kumar, A.; Suban, S. K.; Sahoo, K.; *Spectrochim. Acta, Part A* **2018**, *204*, 105.

5. Gao, M.; Tang, B. Z.; *ACS Sens.* **2018**, *3*, 920.

6. Wang, J.; Li, Y.; Li, K.; Meng, X.; Hou, H.; *Chem. - Eur. J.* **2017**, *23*, 5081.

7. Wang, P.; Wu, X.; Wu, J.; Liao, Y.; *J. Photochem. Photobiol., A* **2019**, *382*, 111929.

8. Hambidge, K. M.; Casey, C. E.; Krebs, N. F. In *Trace Elements in Human and Animal Nutrition*, 5th ed.; Mertz, W., ed.; Academic Press: San Diego, 1986, p. 1-137.

9. Wastney, M. E.; Aamodt, R. L.; Rumble, W. F.; Henkin, R. I.; *Am. J. Physiol.* **1986**, *251*, 398.

10. Kay, R. G.; Tasman-Jones, C.; *Aust. N. Z. J. Surg.* **1975**, *45*, 325.

11. Machado, I.; Bergmann, G.; Pistón, M.; *Food Chem.* **2016**, *194*, 373.

12. Iesari, F.; Trapananti, A.; Minicucci, M.; Filipponi, A.; Di Cicco, A.; *Nucl. Instrum. Methods Phys. Res., Sect. B* **2017**, *411*, 68.

13. Santos, A. B.; Kohlmeier, K. A.; Rocha, M. E.; Barreto, G. E.; Barreto, J. A.; de Souza, A. C. A.; Bezerra, M. A.; *J. Trace Elem. Med. Biol.* **2018**, *47*, 134.

14. Fréchette-Viens, L.; Hadioui, M.; Wilkinson, K. J.; *Talanta* **2019**, *200*, 156.

15. Petrović, S.; Guzsvány, V.; Ranković, N.; Beljin, J.; Rončević, S.; Dalmacija, B.; Ashrafi, A. M.; Kónya, Z.; Švancara, I.; Vytřas, K.; *Microchem. J.* **2019**, *146*, 178.

16. Li, K.; Wang, J.; Li, Y.; Si, Y.; Tang, B. Z.; *Sens. Actuators, B* **2018**, *274*, 654.

17. Czarnik, A. W.; *Fluorescent Chemosensors for Ion and Molecule Recognition*, 1st ed.; American Chemical Society: Washington, 1992.

18. Xu, Z.; Yoon, J.; Spring, D. R.; *Chem. Soc. Rev.* **2010**, *39*, 1996.

19. Liu, Y.; Li, Y.; Feng, Q.; Li, N.; Li, K.; Hou, H.; Zhang, B.; *Luminescence* **2018**, *33*, 29.

20. Wang, P.; Zhou, D.; Chen, B.; *Spectrochim. Acta, Part A* **2018**, *204*, 735.

21. Li, W.; Liu, Z.; Fang, B.; Jin, M.; Tian, Y.; *Biosens. Bioelectron.* **2020**, *148*, 111666.

22. Shirbhate, M. E.; Jeong, Y.; Ko, G.; Baek, G.; Kim, G.; Kwon, Y.-U.; Kim, M. K.; Yoon, J.; *Dyes Pigm.* **2019**, *167*, 29.

23. Hu, Z.; Yang, G.; Hu, J.; Wang, H.; Eriksson, P.; Zhang, R.; Zhang, Z.; Uvdal, K.; *Sens. Actuators, B* **2018**, *264*, 419.

24. Wang, P.; Wu, J.; An, Y.; Liao, Y.; *Spectrochim. Acta, Part A* **2019**, *220*, 117140.

25. Zhang, Y.-P.; Xue, Q.-H.; Yang, Y.-S.; Liu, X.-Y.; Ma, C.-M.; Ru, J.-X.; Guo, H.-C.; *Inorg. Chim. Acta* **2018**, *479*, 128.

26. Kumar, S. S.; Kumar, R. S.; Ashok, S. K.; *Inorg. Chim. Acta* **2020**, *502*, 119348.

27. Lin, H. Y.; Chen, T. Y.; Liu, C. K.; Wu, A. T.; *Luminescence* **2016**, *31*, 236.

28. Patil, M.; Bothra, S.; Sahoo, S. K.; Rather, H. A.; Vasita, R.; Bendre, R.; Kuwar, A.; *Sens. Actuators, B* **2018**, *270*, 200.

29. Naik, K.; Revankar, V.; *J. Fluoresc.* **2018**, *28*, 1105.

30. Jonaghani, Z. M.; Zali-Boeini, J. H.; Moradi, H.; *Spectrochim. Acta, Part A* **2019**, *207*, 16.

31. Feng, Q.; Li, Y.; Li, K.; Lu, J.; Wang, J.; Fan, P.; Li, D.; Wu, D.; Hou, H.; *ChemistrySelect* **2017**, *2*, 3158.

32. Hosseini, M.; Vaezi, Z.; Ganjali, M. R.; Faridbod, F.; Abkenar, S. D.; Alizadeh, K.; Salavati-Niasari, M.; *Spectrochim. Acta, Part A* **2010**, *75*, 978.

33. Li, Y.; Li, K.; He, J.; *Talanta* **2016**, *153*, 381.

34. Aziz, A. A. A.; Seda, S. H.; *Sens. Actuators, B* **2014**, *197*, 155.

35. Aziz, A. A. A.; Seda, S. H.; *J. Fluoresc.* **2015**, *25*, 1711.

36. Aziz, A. A. A.; Mohamed, R. G.; Elantabli, F. M.; El-Medani, S. M.; *J. Fluoresc.* **2016**, *26*, 1927.

37. Aziz, A. A. A.; Seda, S. H.; Mohammed, S. F.; *Sens. Actuators, B* **2016**, *223*, 566.

38. Schwarzenbach, G.; Flaschka, H.; *Complexometric Titrations*, 2nd ed.; Methuen: London, 1969, p. 260.

39. Mohamed, R. G.; Makhlouf, A. A.; Mosad, S. A.; Aziz, A. A. A.; El-Medani, S. M.; Ramadan, R. M.; *J. Coord. Chem.* **2018**, *71*, 3665.

40. Williams, A. T. R.; Winfield, S. A.; Miller, J. N.; *Analyst* **1983**, *108*, 1067.

41. Parker, C. A.; Rees, W. T.; *Analyst* **1960**, *85*, 587.

42. Crosby, G. A.; Demas, J. N.; *J. Phys. Chem.* **1971**, *75*, 991.

43. Zhou, X.; Yu, B.; Guo, Y.; Tang, X.; Zhang, H.; Liu, W.; *Inorg. Chem.* **2010**, *49*, 4002.

44. Aziz, A. A. A.; *J. Lumin.* **2013**, *143*, 663.

45. Wen, J.; Geng, Z.; Yin, Y.; Zhang, Z.; Wang, Z.; *Dalton Trans.* **2011**, *40*, 1984.

46. Long, G. L.; Winefordner, J. D.; *Anal. Chem.* **1983**, *55*, 712A.

47. Jiao, Y.; Zhu, B.; Chen, J.; Duan, X.; *Theranostics* **2015**, *5*, 173.

48. Sadia, M.; Naz, R.; Khan, J.; Khan, R.; *J. Fluoresc.* **2018**, *28*, 1281.

49. Wang, J.; Qian, X.; Cui, J.; *J. Org. Chem.* **2006**, *71*, 4308.

50. Vosburgh, W. C.; Copper, G. R.; *J. Am. Chem. Soc.* **1941**, *63*, 437.

51. Benesi, H. A.; Hildebrand, J. H.; *J. Am. Chem. Soc.* **1949**, *71*, 2703.

52. Ahumada, M.; Lissi, E.; Montagut, A. M.; Valenzuela-Henríquez, F.; Pacioni, N. L.; Alarcon, E. I.; *Analyst* **2017**, *142*, 2067.

53. Conners, K. A.; *Binding Constants - The Measurement of Molecular Complex Stability*; John Wiley & Sons: New York, 1987.

54. Li, Y.; Wu, J.; Jin, X.; Wang, J.; Han, S.; Wu, W.; Xu, J.; Liu, W.; Yao, X.; Tang, Y.; *Dalton Trans.* **2014**, *43*, 1881.

55. Budri, M.; Chimmalagi, G.; Naik, G.; Patil, S.; Gudasi, K.; Inamdar, S.; *J. Fluoresc.* **2019**, *29*, 1065.

56. Aziz, A. A. A.; Seda, S. H.; *J. Fluoresc.* **2017**, *27*, 1051.

57. Frisch, M. J.; Trucks, G. W.; Schlegel, H. B.; Scuseria, G. E.; Robb, M. A.; Cheeseman, J. R.; Montgomery Jr., J. A.; Vreven, T.; Kudin, K. N.; Burant, J. C.; Millam, J. M.; Iyengar, S. S.; Tomasi, J.; Barone, V.; Mennucci, B.; Cossi, M.; Scalmani, G.; Rega, N.; Petersson, G. A.; Nakatsuji, H.; Hada, M.; Ehara, M.; Toyota, K.; Fukuda, R.; Hasegawa, J.; Ishida, M.; Nakajima, T.; Honda, Y.; Kitao, O.; Nakai, H.; Klene, M.; Li, X.; Knox, J. E.; Hratchian, H. P.; Cross, J. B.; Bakken, V.; Adamo, C.; Jaramillo, J.; Gomperts, R.; Stratmann, R. E.; Yazyev, O.; Austin, A. J.; Cammi, R.; Pomelli, C.; Ochterski, J. W.; Ayala, P. Y.; Morokuma, K.; Voth, G. A.; Salvador, P.; Dannenberg, J. J.; Zakrzewski, V. G.; Dapprich, S.; Daniels, A. D.; Strain, M. C.; Farkas, O.; Malick, D. K.; Rabuck, A. D.; Raghavachari, K.;

Foresman, J. B.; Ortiz, J. V.; Cui, Q.; Baboul, A. G.; Clifford, S.; Cioslowski, J.; Stefanov, B. B.; Liu, G.; Liashenko, A.; Piskorz, P.; Komaromi, I.; Martin, R. L.; Fox, D. J.; Keith, T.; Al-Laham, M. A.; Peng, C. Y.; Nanayakkara, A.; Challacombe, M.; Gill, P. M. W.; Johnson, B.; Chen, W.; Wong, M. W.; Gonzalez, C.; Pople, J. A.; *Gaussian 03, Revision C.02*; Gaussian, Inc., Wallingford, CT, 2004.